Applied Energy 361 (2024) 122884

Contents lists available at ScienceDirect

Applied Energy

journal homepage: www.elsevier.com/locate/apenergy

Techno-economic and environmental analyses of hybrid renewable energy systems for a remote location employing machine learning models

Dibyendu Roy [a], Shunmin Zhu [a,*], Ruiqi Wang [a], Pradip Mondal [b], Janie Ling-Chin [a], Anthony Paul Roskilly [a]

[a] *Department of Engineering, Durham University, Durham DH1 3LE, UK*
[b] *Department of Mechanical Engineering, Indian Institute of Engineering Science and Technology, Shibpur, Howrah, West Bengal 711103, India*

HIGHLIGHTS

- Four different configurations of hybrid renewable energy systems are considered.
- The configuration that integrated PV, wind turbine, biogas generator, battery, and converter is best.
- Machine learning techniques are used to assess economic and environmental performances.
- The bilayered neural network, with ReLU activation function, outperforms other models in predicting LCOE with $R^2 = 1$
- The medium neural network, using ReLU activation, outperforms other models in predicting CO_2 emissions with $R^2 = 1$.

ARTICLE INFO

Keywords:
Energy conversion
Hybrid renewable energy system
Levelized cost of electricity
Machine learning
Techno-economic analysis

ABSTRACT

This article offers a detailed investigation into the technical, economic along with environmental performance of four configurations of hybrid renewable energy systems (HRESs), aiming at supplying renewable electricity to a remote location, Henry Island in India. The study explores combinations involving photovoltaic (PV) panels, wind turbines, biogas generators, batteries, and converters, while evaluating their economic, technical, and environmental performance. The economic analysis yield that among all the systems examined, the PV, wind turbine, biogas generator, battery, and converter integrated configuration stands out with highly favourable results, showcasing the minimal value of levelized cost of electricity (LCOE) at $0.4224 per kWh and the lowest net present cost (NPC) at $6.41 million. However, technical analysis yield that the configuration comprising wind turbines, PV panels, converters, and battery yields a maximum excess electricity output of 2,838,968 kWh/yr. Additionally, machine learning techniques are employed to analyse economic and environmental performance data. The study shows Bilayered Neural Network model achieves exceptional accuracy in predicting LCOE, while the Medium Neural Network model proves to be the most accurate in predicting environmental performance. These findings provide valuable perception into the design and optimisation of HRES systems for off-grid applications in remote regions, taking into account their technical, economic, and environmental aspects.

1. Introduction

1.1. Background and motivation

Energy consumption in India has doubled since 2000, primarily relying on coal, oil, and solid biomass to fulfil 80% of the demand [1]. The country emits 1.5 Mt./TWh of CO_2 emissions from fuel combustion per unit of the total electricity output [2]. Currently, solar energy contributes less than 4% to India's electricity generation, while coal accounts for approximately 70% [1]. Although there has been significant growth in renewable energy sources, particularly in solar power, there is still much work to be done to fulfil India's commitment to reaching 450 GW of renewable capacity by 2030 [3] and achieving the Net Zero target [4].

Rural areas in India, where a significant portion of the population resides, often face challenges in accessing reliable and uninterrupted electricity [5]. The challenges faced in remote areas are considerable. Despite government efforts to bring electricity to these regions, frequent power outages hinder consistent and uninterrupted access to power. In

* Corresponding author.
E-mail addresses: dibyendu.roy@durham.ac.uk (D. Roy), shunmin.zhu@durham.ac.uk (S. Zhu).

https://doi.org/10.1016/j.apenergy.2024.122884
Received 26 September 2023; Received in revised form 17 January 2024; Accepted 16 February 2024

Nomenclature

Abbreviations

BG	biogas generator
CAP	capital cost
CRF	capital recovery factor
DG	diesel generator
EM	CO_2 emission
FT	fixed tilt
GPR	Gaussian process regression
HDA	horizontal daily adjustment
HMA	horizontal monthly adjustment
HRES	hybrid renewable energy systems
LCA	life cycle assessment
LCOE	levelized cost of electricity,$/kWh
MAE	mean absolute error
MCDM	multi-criteria decision-making
ML	machine learning
MSE	mean square error
NPC	net present cost, $
OM	operating and maintenance cost, $
PHES	pumped hydro energy storage
PV	photovoltaic
RC	replacement cost,$
RMSE	root mean square error
SL	salvage cost,$
STC	standard test conditions
SVM	support vector machines
VCA	vertical continuous adjustment
WT	wind turbines

Symbols

C_{annual}	total annualised cost, $
d_n	real discount rate
E_{GEN}	total annual electricity, kWh
E_{PV}	energy from the PV arrays, kWh
f_r	rate of inflation,%
FD_{PV}	derating factor of PV
I_T	incident solar irradiation on the PV array, W/m^2
$I_{T,STC}$	incident solar irradiation at the STC, W/m^2
LHV_{fuel}	lower heating value of the fuel, MJ/kg
m_{fuel}	mass flow rate of fuel, kg/s
N_k	the number of components
P_{BG}	power output of the generator, kW
$T_{a,NOCT}$	ambient temperature, °C
T_C	temperature of the PV cell, K
$T_{C,NOCT}$	operating (nominal) cell temperature, °C
$T_{C,STC}$	temperature of the cell under STC, K
T_k	lifetime of component, year
$T_{k,rem}$	remaining lifespan of the kth component, year
$T_{Pro,j}$	lifetime of the project, year
V	velocity, m/s
$V_{cut,in}$	cut-in wind speed, m/s
$V_{cut,off}$	cut-off wind speed, m/s
V_{rated}	rated wind velocity, m/s
W_{PV}	power output of a photovoltaic array, kW
W_{rated}	rated power, kW
W_{WT}	power delivered by the wind turbines, kW
Z_{PV}	rated capacity of PV array, kW
Δt	time-period, hour

Greek letters

β_t	temperature coefficient of power
η_{BG}	electrical efficiency of the BG
$\eta_{MP,STC}$	maximum power efficiency achieved under STC

Subscripts

k	the kth component

this regard, integration of various renewable energy resources such as solar, biomass, and wind through hybridization employing hybrid renewable energy systems (HRES), presents a promising solution for rural and remote areas.

1.2. Review of literature

Numerous studies have been undertaken to evaluate the technical and financial viability of HRES across various nations. Abdelhady [6] investigated various configurations of HRES that integrate photovoltaic (PV), wind turbine (WT), converter, and biogas generator (BG) with the electric grid employing technoeconomic analysis. The study focused on a hotel located in a typical city in Egypt. The findings revealed that the PV/WT grid-connected system would exhibit the minimal value of net present cost (NPC) of 388 k$ and levelized cost of electricity (LCOE) of 0.021 $/kWh. Das et al. [7] examined HRES incorporating solar and small hydro energy, diesel generator, as well as storage modules to deliver affordable continuous power using technoeconomic analysis. By comparing five storage modules (lead acid, lithium-ion, vanadium redox and zinc bromide batteries, and pumped hydro energy storage (PHES)) across two distinct strategies, they determined that the optimal solution would have a LCOE of $0.197/kWh and NPC of $3,62,384. Mulumba and Farzaneh [8] examined the use of HRES in a remote area of Makueni County, Kenya using technoeconomic analysis and multi objective optimisation techniques. The system integrated PV and WT technologies, along with a storage facility that combined lithium-ion batteries and a flywheel storage system and found that the LCOE was significantly reduced to $0.519 per kWh. Similarly, Ahmed et al. [9] examined HRES configuration in Al-Issawiya, Sudan employing technoeconomic and environmental analyses. The system combined PV panels, diesel generator system, and an energy storage with a solar tracking system. The study leading to an optimal LCOE of $0.18 per kWh. In another study, Das and De [10] investigated HRES configurations that integrated WT, PV, convertor, diesel generator, and battery storage in a remote village in Gujarat using technoeconomic analysis, multi-criteria decision-making (MCDM), and life cycle assessment (LCA). Their optimal solution for the village would be a combination of PV, diesel generator, and battery systems, resulting in a LCOE of $0.21 per kWh. Ma and Javed [11] analysed HRES consisting of PV, battery, WT, along with convertor components for the remote island of Jiuduansha, China using technoeconomic analysis. They reported that a WT-only system achieved a minimum LCOE of $0.187 per kWh. Skroufouta and Baltas [12] investigated on HRES configuration that integrated WT, PV, and a desalination plant in the remote area of Karpathos island, Greece. They found that the system was reliable, and could fulfil the drinking water requirements of the island, 89.75% of irrigation needs, and 50.63% of energy demands. Yazdani et al. [13] conducted a comprehensive examination of various off-grid and on-grid configurations for HRES using environmental analysis and a MCDM algorithm to determine the optimal design configuration. They reported that the configuration comprising PV, FC, electrolyser, hydrogen tank, Battery and Inverter, with a 20% grid integration for the on-grid scenario, emerged as the most prominent configuration. Dehshiri and Firoozabadi [14] explored the integration of PV and converter components in a grid-connected HRES in Iran. Their investigation utilised technoeconomic analysis and MCDM techniques to evaluate the feasibility of various PV system configurations, including fixed tilt, vertical continuous adjustment, horizontal monthly adjustment, and horizontal daily adjustment. Their findings indicated that the fixed tilt system exhibited the lowest LCOE, with this parameter reported to be 0.097 $/kWh.

Machine learning models can be effective tools for measuring performance investigations of HRES configurations. It has been applied to medical diagnosis [15], transient emission prediction of diesel engine [16], financial crisis prediction [17], Coronavirus disease prediction [18], and crude oil price prediction [19]. However, very few studies can be found on HRES system where machine learning techniques were employed. Shabestari et al. [20], predicted of future power outages in rural areas of Iran using machine learning techniques with various linear regression models focusing on a grid connected HRES comprising PV panels, a biodiesel fuelled generator, and a battery bank. They considered three power outage scenarios: peak-time outages, planned outages, and random outages, showing that LCOE would range between $0.066/kWh and $0.070/kWh while maintaining an optimal hybrid solution with a renewable energy share of approximately 15%. Roy [21] examined off-grid HRES configurations comprising diesel fuelled generators, WTs, PV panels, converters, and batteries on a remote Indian island using machine learning techniques. The findings indicated that would be the most efficient configuration offering minimum LCOE of $0.31 per kWh. Izadi et al. [22] used a genetic algorithm-based machine learning approach to optimise an HRES comprising PV, WT, electrolyzer, fuel cell, and control devices. Their study aimed to determine the optimal levels of CO_2 emissions, cost rate, and loss of power supply probability (LPSP). The findings revealed that the optimised system yielded a CO_2 emission of 53.48 tons/year, a low LPSP of 0.4057, and a system cost rate of 1.422 €/hr. In another study, Sakthi et al. [23] employed a support vector machine-based machine learning approach to assess the performance of HRES integrating PV and WT. Employing a support vector machine-based approach, the method demonstrated impressive results with 89% scalability, 86% power consumption, 95% network efficiency, and a high training accuracy of 96%. Ghandehariun et al. [24] explored an HRES incorporating WTs, PVs, electrolysers, pumped-hydro, and reverse osmosis. Using a backpropagation neural network, they predicted the system's exergy efficiency, achieving a high R^2 value of 0.98.

The performance of HRES has been evaluated and optimised by various methodologies, and Table 1 presents a summary of related studies.

1.3. Novelty and contribution of the work

The literature review showed that prior studies on HRES have primarily focused on evaluating the techno-economic performance of these systems via integrating the renewable and non-renewable energy sources, and the application of machine learning techniques in assessing HRES performance has been relatively limited. Whereas there is a gap in research utilising machine learning algorithms to explore the techno-economic and environmental aspects of HRES that incorporate 100% renewable energy sources. This study will make several contributions including:

- Analysing the technical, financial, and environmental aspects of four HRES configurations to electrify a remote island in India. These configurations involve PV panels, WTs, BG, batteries, and converters.
- Determination of the optimal configuration among the developed HRES based on the criteria for achieving the minimal LCOE.
- Utilising component sizes as input data to predict economic and environmental performances, exploring variations in the sizing of PV panels, WT, BG, batteries, and converters—examining 1295 potential combinations. The collected data underwent comprehensive analysis using 26 distinct machine learning models.
- Determining the optimal machine learning model to precisely predict the techno-economic performance parameter, LCOE, as well as the environmental emission performance parameter, CO_2 emissions (EM), for the developed HRES configurations.

2. Material and methods

2.1. Study location and energy availability

The chosen study location is situated in Henry Island near Bakkhali in South 24 Parganas, West Bengal, India and the location is marked in Fig. 1. According to 2011 Census, the island has a total population of

Table 1
Summary of related studies on performance optimisation of HRES.

Combination	Scope	Objective function	Key findings	Location
PV/WT/BG/Flywheel/Battery [25]	Off-grid and on-grid HRES for a governorate	Minimise net present and levelized cost, maximise renewable electricity share by commercial software	PV/WT system connected to the grid with batteries for storage is the optimal configuration	Jordan
PV/WT/Hydro/Battery [26]	Stand-alone HRES for a remote rural area	Optimise cost of energy and net present cost by commercial software	Under combined dispatch strategy, lithium-ion battery based HRES delivers the most optimal operational costs	India
PV/WT/Fuel cells [27]	Stand-alone HRES for a city	Minimise total system cost by Al-Biruni algorithm	The Modified Al-Biruni Earth Radius (MBER) algorithm is found to be the most efficient and reliable system	China
PV/WT/Diesel/Battery [28]	Stand-alone, reliability-constrained HRES	Optimise solution for cost and reliability using robust satisficing approaches	The scenario-based and stochastic-free robust satisficing lead to better in-sample solutions	Canada
PV/WT/Diesel/Battery [29]	Stand-alone HRES	Minimise cost by robust simulation-optimisation methods	The robust model with a properly-sized distributional ambiguity set leads to better solutions than the nominal model	Canada
PV/BG/Battery/Electrolyser/Fuel cells [30]	Renewable-based hydrogen and electricity co-supply hub	Minimise total annual cost and optimise capacity arrangement using metaheuristic-TOPSIS approach	The multi-objective mayfly algorithm assisted with TOPSIS generates the most preferred solution	Malaysia
PV/WT/BG/Battery [31]	Stand-alone HRES for two rural areas	Optimise economic, environmental, technical, and energy security criteria by multi-criteria decision-making	The optimum solution reduces CO_2 emissions by over 20% and yeilds lower fuel dependency	Iran
PV/BG/Hydro/Battery [32]	On-grid HRES for a village	Optimise techno-economic solution for HRES by a Fractional order updated JAYA algorithm	The non-reliable power supply from grid can be supported with the designed HRES	India
PV/WT/Diesel/Electrolyser/Fuel cell/Battery [33]	Off-grid HRES for a city	Minimise levelized cost of energy and CO_2 emissions by multi-objective optimisation method based on the Taguchi approach	The hybridization of energy resources allows lower annual emissions compared to a diesel-only system.	Turkey
PV/Battery [34]	On-grid HRES for a commercial centre	Predict weather patterns over the lifespan of a HRES in optimising its size by machine learning and hybrid metaheuristics	The approach leads to a more realistic HRES capacity that satisfies weather conditions over the lifespan of the system	South Korea

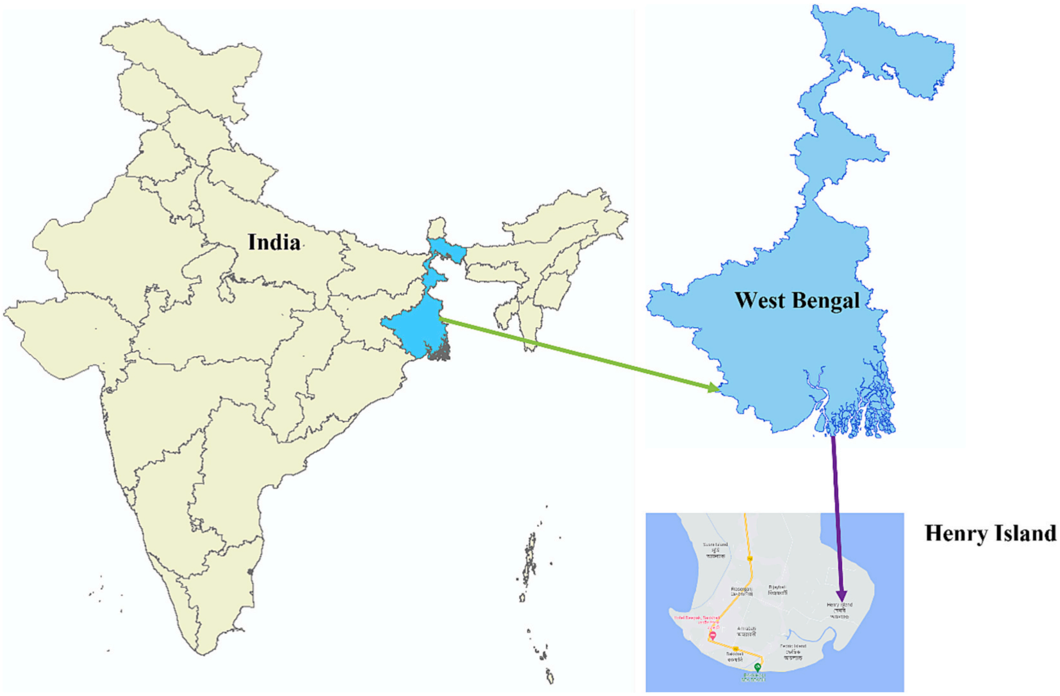

Fig. 1. Study location (*Henry Island, West Bengal, India*).

6675 persons [35]. The present analysis takes into account the energy requirements of 1600 households, as outlined in Table A1 of Appendix A.

Fig. 2 presents the recorded monthly solar irradiation and clearness index at Henry Island obtained from NASA databases [36]. Throughout the year, the monthly solar irradiation ranges between 3.774 kWh/m^2 per day and 5.43 kWh/m^2 per day, with an estimated average solar irradiation of 4.506 kWh/m^2 per day. April exhibits the highest levels of solar irradiation, whereas July experiences the lowest intensity. The clearness index is derived by dividing the amount of global irradiation received at the Earth's surface on a horizontal plane by the corresponding extraterrestrial irradiation on a horizontal plane during the same time period [37]. This dimensionless parameter ranges from 0 to 1, with higher values indicating clearer skies. Notably, the clearness index reaches its lowest point of 0.344 in July and peaks at its highest level of 0.568 in December. The wind speed data for the study area, also sourced from NASA databases [36], is depicted in Fig. 3. Wind speed, ranging from 3.77 m/s to 7.44 m/s on Henry Island, substantially impacts WT power output, with the importance of optimising cut-in and cut-out speeds and selecting suitable sites based on local wind patterns to maximise energy output. Furthermore, the location has a steady supply of woody biomass which can be used in the biomass systems. Fig. 4 illustrates the average available biomass on a daily basis [38], as shown on the left axis, along with the average temperature at the location, displayed on the right axis.

2.2. System topology

This study focuses on the performance optimisation of four different hybrid energy systems that operate entirely on renewable sources. The proposed configurations of these systems involve the integration of solar, wind, biomass, converter, and battery technologies. The system

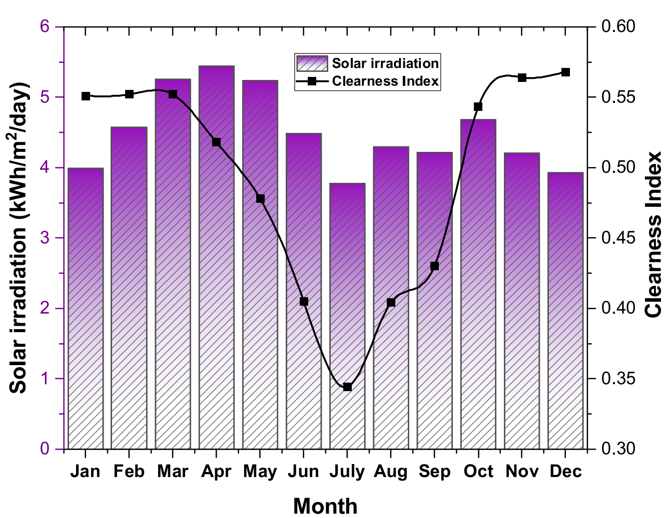

Fig. 2. Solar irradiation and Clearness Index of Henry Island, West Bengal, India.

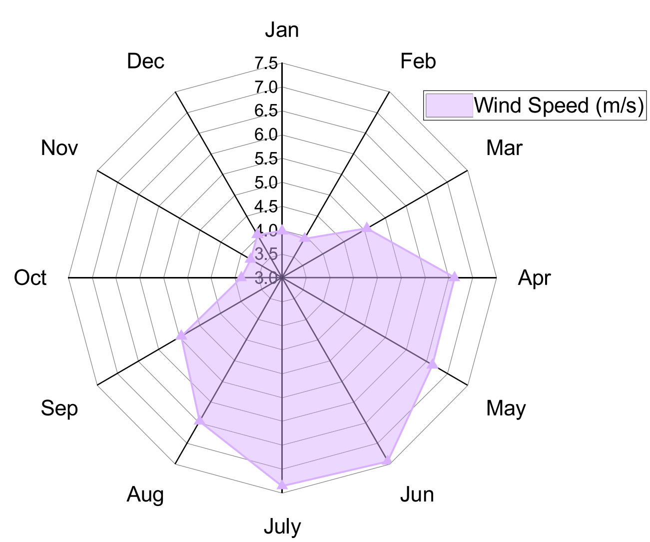

Fig. 3. Monthly wind speed at the location.

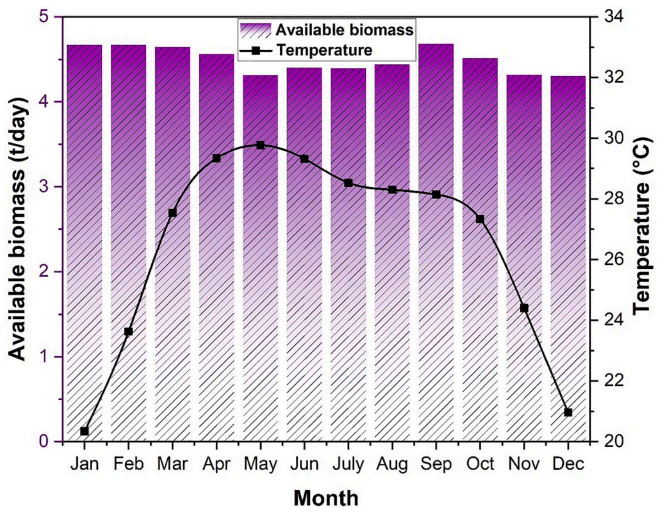

Fig. 4. Daily average available biomass and average temperature at the location.

configurations are modelled to meet the required electricity demand throughout the year, with a simulation time step of 1 h. The details of the system configurations are provided below.

- System A: PV, WT, BG, convertor, battery integrated system
- System B: PV, BG, convertor, battery integrated system
- System C: WT, PV, convertor, battery integrated system
- System D: WT, BG, convertor, battery integrated system

The diagrams illustrating the suggested configurations are presented in Fig. 5.

2.3. Energy performance of the system components

2.3.1. Photovoltaic array

The power output of a photovoltaic array is denoted by $\dot{W}_{PV}$ (kW) and it can be determined as follows [39]:

$$\dot{W}_{PV} = Z_{PV} \times FD_{PV} \times \left(\frac{\overline{I_T}}{\overline{I}_{T,STC}}\right) \times \left(1 + \beta_t\left(T_C - T_{C,STC}\right)\right) \tag{1}$$

where Z_{PV}: rated capacity of PV array (kW), FD_{PV}: derating factor of PV (%), $\overline{I_T}$: Incident solar irradiation on the PV array during the present time step (kW/m^2), $\overline{I}_{T,STC}$: incident solar irradiation at the standard test conditions (STC) (kW/m^2), β_t: temperature coefficient of power, T_C: temperature of the PV cell at the present time step (°C) and, $T_{C,STC}$: temperature of the cell under STC (°C).

To estimate the PV cell temperature, the following equation can be utilised [39]:

$$T_c = \frac{T_a + \left(T_{C,NOCT} - T_{a,NOCT}\right)\left(\frac{\overline{I_T}}{\overline{I}_{T,STC}}\right)\left(1 - \frac{\eta_{MP,STC}\left(1-\beta_t \times T_{C,STC}\right)}{\tau\alpha}\right)}{1 + \left(T_{C,NOCT} - T_{a,NOCT}\right)\left(\frac{\overline{I_T}}{\overline{I}_{T,STC}}\right)\left(\frac{\beta_t \times \eta_{MP,STC}}{\alpha\tau}\right)} \tag{2}$$

where $T_{C,NOCT}$ and $T_{a,NOCT}$ denote the nominal operating cell temperature (NOCT) and ambient temperature, respectively. The NOCT is considered as 20 °C. The parameter $\eta_{MP,STC}$ denotes the maximum power efficiency achieved under STC.

Energy converted from the PV arrays is denoted by E_{PV} (kWh) and it can be determined as follows [39]:

$$E_{PV} = N_{PV} \times \dot{W}_{PV}(t) \times \Delta t \tag{3}$$

where, N_{PV} is number of PV arrays; Δt: time-period and is 1 h.

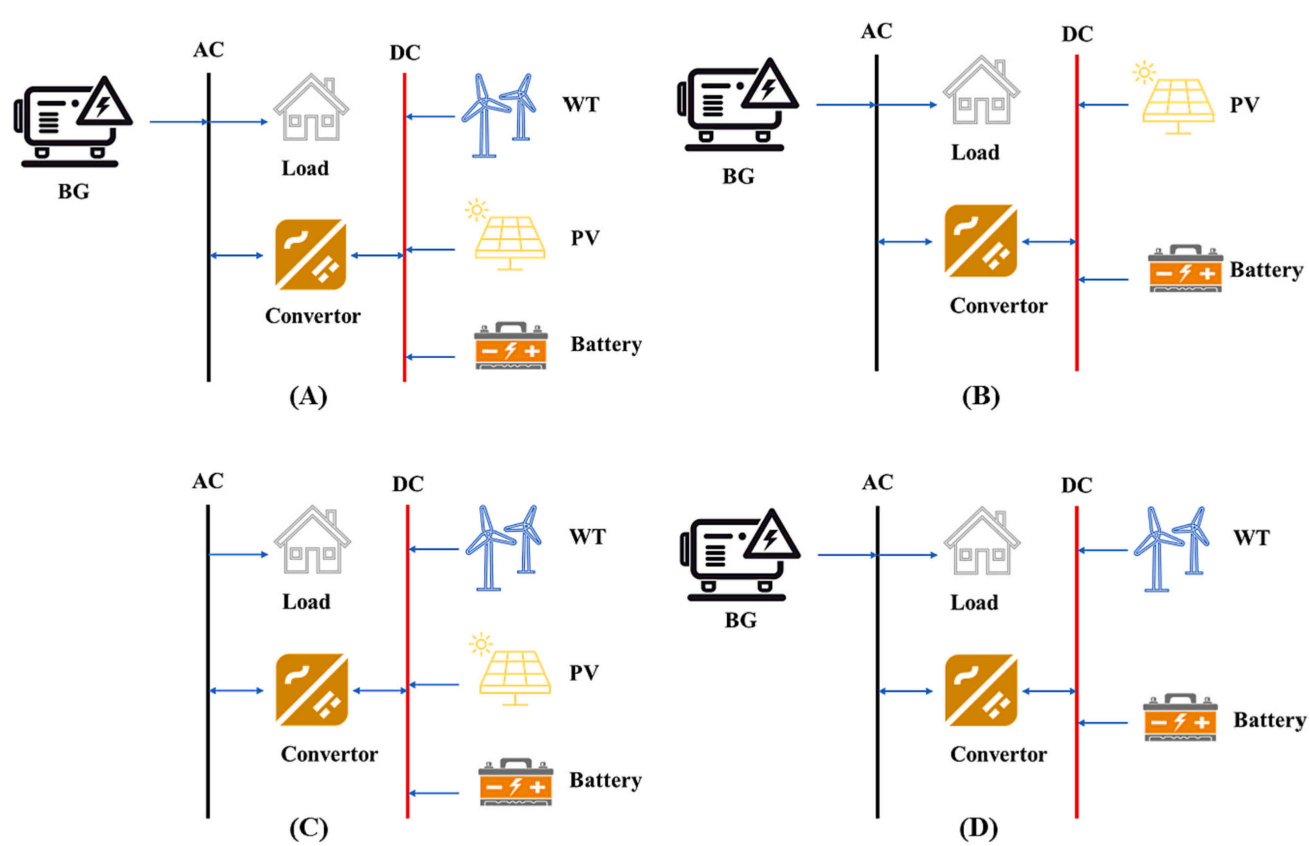

Fig. 5. Topology of the HRES: (A) System A, (B) System B, (C) System C, (D) System D.

2.3.2. Wind turbine (WT)

Power delivered by the WTs is denoted $\overline{W}_{WT}$ (kW) and it can be calculated as follows [40]:

$$\overline{W}_{WT} = \left\{ \begin{array}{c} 0; V < V_{cut,in} \\ \alpha \times V^3 - \beta \times \dot{W}_{rated}; V_{cut,in} < V < V_{rated} \\ \dot{W}_{rated}; V_{rated} < V < V_{cut,off} \\ 0; V > V_{cut,off} \end{array} \right\} \quad (4)$$

where $V_{cut,in}$ (m/s) denotes the cut-in wind velocity, $V_{cut,off}$(m/s) denotes cut-off wind velocity, V_{rated} (m/s) denotes to the rated wind velocity, and $\dot{W}_{rated}$ (kW) denotes the rated power.

The provided equations can be used to determine the values of both 'α' and 'β' [39].

$$\alpha = \frac{\dot{W}_{rated}}{V^3_{rated} - V^3_{cut,in}} \quad (5)$$

$$\beta = \frac{V^3_{cut,in}}{V^3_{rated} - V^3_{cut,in}} \quad (6)$$

2.3.3. Battery

Reliability of any energy system can be improved by integrating battery storage facilities [41]. These facilities are commonly used to supply electrical energy during peak load hours or when renewable sources are unavailable. In this study, lead-acid batteries were assessed for their ability to store surplus energy during the charging process.

The electric energy storage (EES) charge is denoted by Q_{ESS} (kWh) and it can be estimated by the following Eq. [42].

$$Q_{ESS} = Q_{ESS,0} + \int_0^t V_{BAT} I_{BAT} dt \quad (7)$$

where, $Q_{ESS,0}$ is the initial EES charge (kWh), V_{BAT} is the battery voltage (V), and I_{BAT} is battery current (A).

The batteries state of charge (SOC) can be estimated by the following Eq. [42].

$$BAT_{SOC} = \frac{Q_{ESS}}{Q_{ESS,max}} \times 100 \quad (8)$$

where $Q_{ESS,max}$ is the total EES's capacity (kWh).

2.3.4. Biogas generator (BG)

Electrical efficiency of the BG is denoted by η_{BG} (%) and it can be calculated as follows [43]:

$$\eta_{BG} = \frac{3.6 \times P_{BG}}{\dot{m}_{fuel} \times LHV_{fuel}} \quad (9)$$

where,$\dot{m}_{fuel}$:mass flow rate of fuel (kg/h),P_{BG}:power output of the generator (kW), and LHV_{fuel}:lower heating value of the fuel (MJ/kg).

2.4. Economics of the configurations

Economic performance of the proposed configurations has been investigated using two important indicators: (i) net present cost (NPC) and (ii) levelized cost of energy (LCOE). The total NPC ($) was calculated using the following mathematical expression [44,45]:

$$NPC = CAP + OM + RC + SL \quad (10)$$

where different cost components like capital costs, operating and maintenance costs, replacement costs, and salvage costs, are termed as CAP ($), OM ($), RC ($), and SL ($), respectively. The costs for different components of the four considered systems can be found in in Table A2 of Appendix A.

During the calculation of capital cost (CAP) of the configurations, the number of components (N_k) is multiplied by the corresponding capital cost of the kth component (CAP_k) and can be determined as follows [44]:

$$CAP = \sum_{k=1}^{Ncomp} N_k CAP_k \quad (11)$$

Operating and maintenance cost (OM) is determined as follows [44]:

$$OM = \sum_{k \in comp} \sum_{y=1}^{T_{Proj}} \frac{1}{\left[1 + \left(\frac{d_n - f_r}{1+f_r}\right)\right]^y} N_k \times OM_k \quad (12)$$

where OM_k: operating and management cost any (kth) component ($), d_n: real discount rate (%), f_r: rate of inflation (%), and T_{Proj}: lifetime of the project in years.

The replacement cost (RC) of any component can be computed as follows [44]:

$$RC = \sum \frac{1}{\left[1 + \left(\frac{d_n - f_r}{1+f_r}\right)\right]^{T_k}} N_k \times RC_k \quad (13)$$

where T_k: total lifetime of any component (in years), and RC_k: total replacement cost ($).

Now, the total salvage cost (SL) can be estimated as follows [44]:

$$SL = \sum_{k \in comp} \frac{1}{\left[1 + \left(\frac{d_n - f_r}{1+f_r}\right)\right]^{T_k}} \times \frac{T_{k,rem}}{T_k} \times N_k \times SL_k \quad (14)$$

where $T_{k,rem}$: remaining lifespan of the kth component, and SL_k: salvage cost ($).

Total annualised cost (C_{annual}) is estimated as follows:

$$C_{annual} = NPC \times CRF \quad (15)$$

where CRF: capital recovery factor and it is determined as:

$$CRF = \frac{\left(\frac{d_n - f_r}{1+f_r}\right) \times \left[1 + \left(\frac{d_n - f_r}{1+f_r}\right)\right]^p}{\left[1 + \left(\frac{d_n - f_r}{1+f_r}\right)\right]^{T_{Pro}} - 1} \quad (16)$$

2.5. Objective function and optimisation constraints

The objective function considered for the analysis is LCOE ($/kWh), representing the minimum cost required to sell the electrical energy to the consumers at break-even price throughout the lifespan of the different HRES. Mathematically, it can be determined as follows [44]:

$$LCOE = \frac{C_{annual}}{E_{GEN}} \quad (17)$$

where C_{annual}: total annualised cost ($), and E_{GEN}:total annual electricity (kWh).The HRES is optimised to meet the necessary electrical demand while minimising the LCOE, subject to specified optimisation constraints. These constraints are outlined below.

a) Range of decision variables: The decision variables for optimising the size of the HRES are determined by the various components it comprises. In order to facilitate efficient computations, predefined upper and lower bounds are imposed on the solution space, outlined as follows:

$$N_{m,min} \le N_m \le N_{m,max}, m \in (\ PV, WT, BG, Convertor, Battery) \quad (18)$$

where N_m represents the number of a system component of m, and $N_{m,min}$ and $N_{m,max}$ refer to the minimum and maximum number of system component of m, respectively.The imposition of upper and lower bounds is implemented to restrict the solution space, effectively reducing processing time. This decision is reached early in the optimisation process, following a trial-and-error approach.

b) Energy balance constraints: The aggregate energy output from all system components within an hour should be equal to or exceed the hourly load demand.

$$E_{PV}(t)+E_{WT}(t)+E_{BG}(t)+E_{ES}(t)\geq E_L(t) \tag{19}$$

where E_{PV},E_{WT}, and E_{BG} are the energy output from PV (kWh), WT (kWh), and BG (kWh) while meeting the total electrical demand (E_L) and storing energy (E_{ES}) at that hour.

c) Energy storage capacity constraints: The constraint governing the energy storage capacity in the system is as follows:

$$H_{ES,min}<H_{ES}(t)<H_{ES,max} \tag{20}$$

where $H_{ES,min}$ (kWh) and $H_{ES,max}$ (kWh) are the maximum electricity storage.

2.6. Machine learning

In this study, an extensive exploration of component sizing variations, encompassing PV panels, WTs, BGs, batteries, and converters, was conducted using machine learning algorithms. A total of 1295 potential combinations of these components were evaluated to assess their economic and environmental emission performances. The collected data underwent comprehensive analysis using 26 distinct machine learning models within the within the MATLAB environment. To validate the accuracy of the regression models, several evaluation metrics were calculated, such as root mean square error (RMSE), mean square error (MSE), mean absolute error (MAE), and coefficient of determination (R^2). RMSE, a widely used statistical metric, is determined as follows [46]:

$$RMSE=\sqrt{\frac{1}{n}\sum\nolimits_{k=1}^{n}(s_k-\dot{s_k})^2} \tag{21}$$

where, n is sample size, s_k is actual value and $\dot{s_k}$ is predicted value.

The MSE metric quantifies the average of the differences (squared) between the predicted and actual values. Mathematically, it can be expressed as the sum of the squares of the errors divided by the total number of observations, as shown below [46]:

$$MSE=\frac{1}{n}\sum\nolimits_{k=1}^{n}(s_k-\dot{s_k})^2 \tag{22}$$

MAE is the statistical metrics that determines the average extent of the errors between the actual and predicted variations and defined as follows [46]:

$$MAE=\frac{1}{n}\sum\nolimits_{k=1}^{n}|s_k-\dot{s_k}| \tag{23}$$

Coefficient of determination (R^2) is a crucial metric used to assess the accuracy of regression model predicted results. It is defined as the ratio of the variance of the predicted values to the variance of the actual values and considered as most important index to verify the exactness of the regression models predicted results and determined as follows [46]:

$$R^2=1-\frac{\sum_{k=1}^{n}(s_k-\dot{s_k})^2}{\sum_{k=1}^{n}(s_k-\overline{s_k})^2} \tag{24}$$

where, $\overline{s_k}$ is the mean of actual value s_k. If, $R^2=1$, the regression model is having extreme level of accuracy.

3. Results and discussions

3.1. Technical analysis

This section provides a comprehensive analysis of the technical performance of four fully hybrid renewable energy system configurations. The analysis primarily focuses on critical technical parameters, such as the optimised design configuration, excess electricity, electricity production and consumption, capacity shortage, renewable fraction, and total fuel consumption. Detailed technical specifications for each of the four HRESs are presented in Table 2. Notably, System C stands out as it does not include a BG unit, eliminating the need for fuel to operate the system. Furthermore, system C yields highest electricity output, followed by System D, System B and System A, respectively. In comparison, System A exhibits the lowest fuel consumption at 470 tons per year, followed by System B at 644 tons per year, and System D at 1143 tons per year. Additionally, all investigated systems demonstrate minimal capacity shortage. In terms of excess electricity generation, System C provides the highest amount, followed by System D, System B, and System A, respectively. It is important to highlight that a higher excess electricity output leads to greater storage requirements. Therefore, System C has the highest energy storage requirement.

3.2. Economic analysis

Fig. 6 presents a graphical representation of the capital costs for four different system configurations, accompanied by a comprehensive breakdown of the capital expenditures linked to each configuration's specific components. It is worth highlighting that system B demonstrates the lowest total capital cost among all the configurations. In system B, the capital cost distribution is as follows: BG contributes 38.82%, PV contributes 35.42%, battery contributes 22.76%, and convertor contributes 3%. On the other hand, system D has the highest capital cost, primarily due to the WT component, which accounts for the largest capital cost contribution at 55.44%. It is followed by BG at 30.55%, battery at 10.64%, and convertor at 3.37%.

Considering the complete lifespan of integrated energy systems, it is crucial to factor in the replacement needs of individual components. Specifically, the Converter, Battery, and BG components will need to be replaced over time. Upon reviewing Fig. 7, it becomes evident that the battery component incurs the highest cost for replacement among all the systems. System A has the lowest overall replacement cost, with the majority of the cost attributed to battery (94.47%), followed by convertor (5.53%). Furthermore, System D requires the second lowest replacement cost, with battery accounting for the largest proportion (73.02%), followed by BG (21.61%), and convertor (5.37%).

Fig. 8 provides a visual representation of the total operation and management costs for each of the four hybrid renewable energy systems. It is worth noting that system D has the highest total O&M cost, primarily due to the significant contribution from BG (64.13%), followed by WT (30.53%), battery (3.87%), and convertor (1.47%). In contrast, system A has the lowest O&M cost, with BG contributing the most (49.80%), followed by PV (23.60%), WT (14.28%), battery (9.70%), and convertor (2.62%), respectively. Furthermore, Fig. 9 illustrates the fuel costs associated with the various components of the systems. Notably, System C stands out as it does not include a BG unit, eliminating the need for fuel to operate that particular system. System D incurs the highest fuel cost at $1,477,841.62, followed by System A and System B. Additionally, Fig. 10 presents the salvage costs for each system configuration. System C has the lowest salvage cost, followed by system A, system D, and system B, respectively. In system B, battery accounts for the highest salvage cost (50.86%), followed by BG (46.26%), and convertor (2.88%).

Fig. 11 presents the net present cost (NPC) and levelized cost of electricity (LCOE) for the four configurations analysed at the study site. As shown, system A achieves the lowest NPC and LCOE, followed by

Table 2
Technical details of the investigated systems.

Technical Parameters	System A	System B	System C	System D
Optimised design	PV:937 kW WT:340 kW BG: 500 kW Convertor:520 kW Battery: 2888Strings	PV: 1479 kW BG:500 kW Convertor:387 kW Battery:3664 Strings	PV:2902 kW WT:313 kW Convertor:719 kW Battery:5006 Strings	WT:1375 kW BG:500 kW Convertor:552 kW Battery:2177 Strings
Electricity output (kWh/yr)	1,894,776	2,074,793	4,184,860	2,633,977
Electricity consumption (kWh/yr)	1,173,840	1,173,840	1,173,133	1,172,900
Excess Electricity (kWh/yr)	560,508	714,990	2,838,968	1,327,943
Capacity Shortage (%)	0	0.0133	0.0602	0.0801
Total fuel consumption (tons/yr)	470	644	0	1143
RF(%)	100	100	100	100

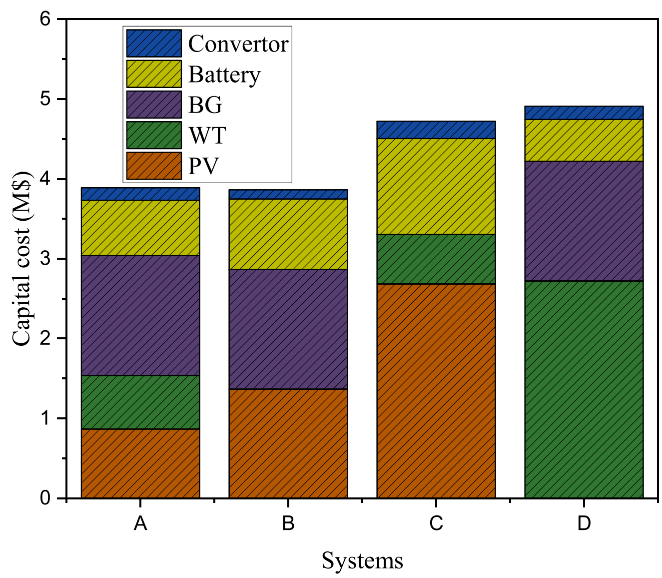

Fig. 6. Capital cost comparison of the four investigated systems.

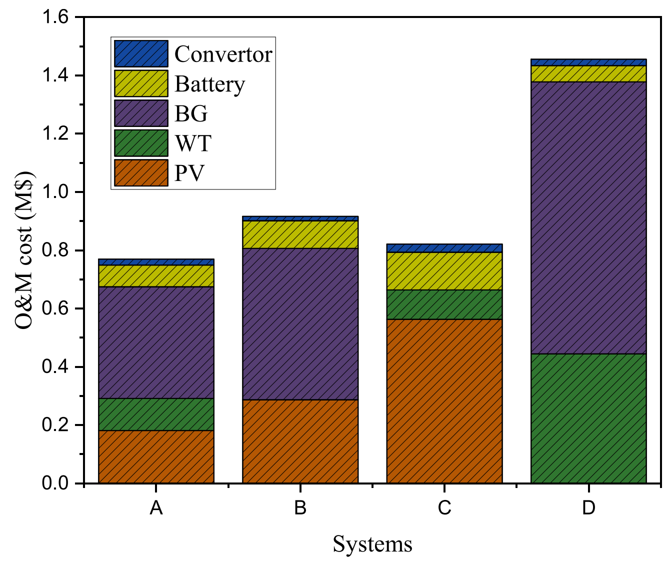

Fig. 8. Operation and management cost comparison of the four investigated systems.

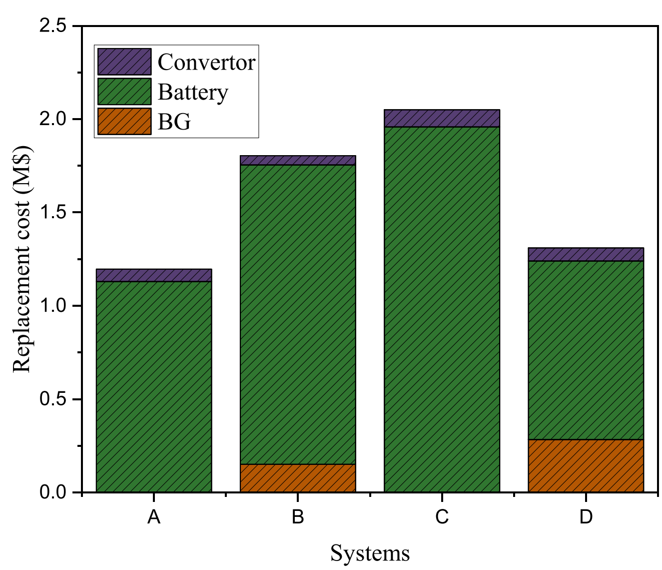

Fig. 7. Replacement cost comparison of the four investigated systems.

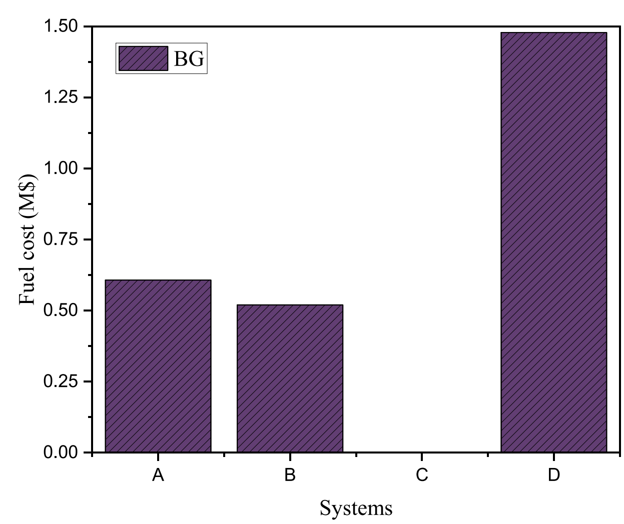

Fig. 9. Fuel cost comparison of the four investigated systems.

system B, system C, and system D, respectively. Specifically, the results indicate that system A, consisting of PV, WT, BG, convertor, battery, has the lowest LCOE (0.4224 $/kWh) and NPC (6.41 M$) among all the systems examined. On the other hand, system D, comprising WT, BG, convertor, battery, exhibits the highest LCOE (0.5947 $/kWh) and NPC (9.02 M$) among all the configurations investigated.

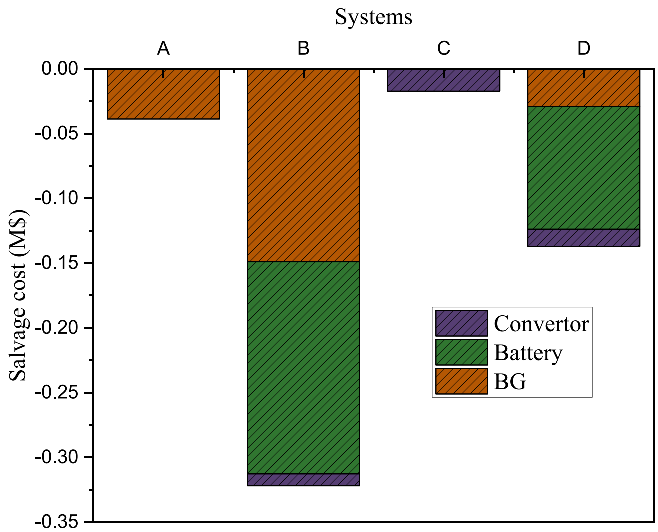

Fig. 10. Salvage cost comparison of the four investigated systems.

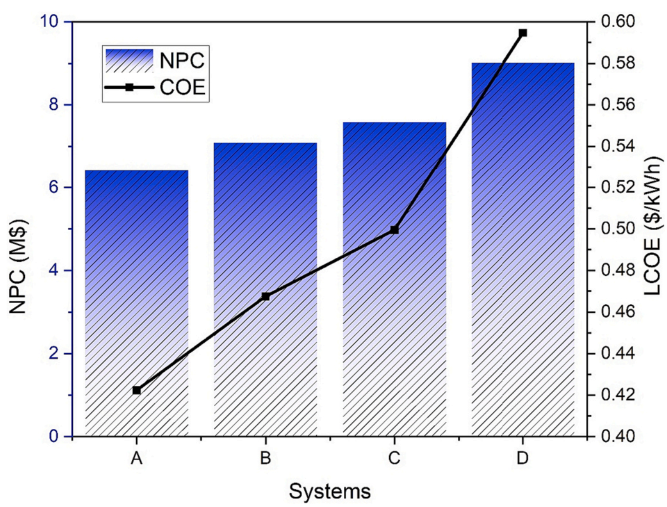

Fig. 11. NPC and LCOE comparison of the four investigated systems.

3.3. Environmental analysis

Fig. 12 provides a comprehensive comparison of CO_2 emissions for the four configurations analysed at the study site. It is important to note that System C, which does not include BG, stands out as an environmentally friendly option, emitting zero CO_2. This makes System C a promising candidate for sustainable practices. Among the remaining three system configurations, System D emerges as the highest emitter of CO_2, releasing a substantial 206 kg/yr. On the other hand, System B and System A exhibit lower CO_2 emissions at 116 kg/yr and 85 kg/yr, respectively.

This data emphasizes the significance of BG in influencing CO_2 emissions, and it showcases the advantages of System C for those seeking to minimise their carbon footprint. Additionally, the results underscore the potential for reducing CO_2 emissions in Systems B and A, suggesting opportunities for further improvement in their design and operation. It is evident from the data that the presence of BG plays a crucial role in reducing carbon emissions, and further research and attention should be directed towards optimising the integration of BG in various configurations.

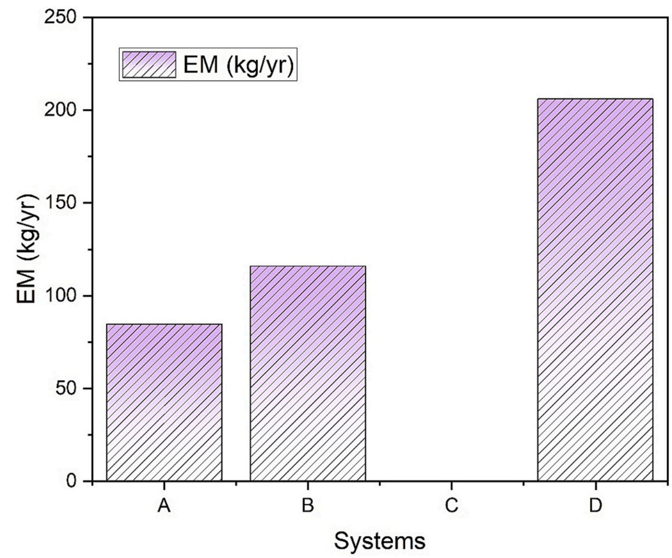

Fig. 12. CO_2 emission comparison of the four investigated systems.

3.4. Data analysis employing machine learning algorithms

The simulation encompassed altering the dimensions of various system elements, including BG capacity, PV capacity, WT capacity, converter capacity, and the number of battery strings, in diverse permutations. This was done to forecast the corresponding LCOE and CO_2 emissions. The data obtained from the energy models is pre-processed and organised in an Excel file for further analysis using machine learning algorithms. Over 1200 combinations of data were thoroughly examined using Machine Learning techniques within the MATLAB environment. The data's attributes are depicted using scatter plots in the scatter matrix plot, as depicted in Fig. 13.

3.4.1. LCOE prediction using machine learning models

A wide range of machine learning techniques, including Linear Regression, Tree, Support Vector Machines (SVM), Ensemble, Gaussian Process Regression (GPR), Neural Network, and Kernel, have been employed to build a predictive model for estimating the LCOE of a given hybrid renewable energy system and are presented in Table 3. Furthermore, to prevent overfitting, a 5-fold cross-validation scheme has been employed.

The majority of machine learning methods employed for LCOE prediction demonstrate strong agreement with simulation data. Notably, the Linear Regression, Tree, Ensemble, Neural Network, and Kernel regression models exhibit relatively short training times compared to other models, with a maximum training time of 23.224 s. Conversely, the Cubic SVM training algorithm requires the longest training duration, clocking in at 90.384 s, followed by the Quadratic SVM at 83.369 s. Gaussian Process Regression models range between 34 and 53 s for training. The Coarse Gaussian SVM boasts the shortest training time among all models, completing in just 2.3184 s.

Among the various models, the Neural Network models, including Exponential GPR, Matern 5/2 GPR, and Rational Quadratic GPR, exhibit increasing accuracy in LCOE prediction, showcasing a coefficient of determination of 1. Notably, the Bilayered Neural Network model attains the highest accuracy among all training algorithms, yielding an impressive R^2 value of 1. It achieves the lowest values for RMSE, MSE, and MAE, which are recorded as 7.4143×10^{-3}, 5.4972×10^{-5}, and 3.4191×10^{-3}, respectively. Thus, the Bilayered Neural Network model emerges as the optimal choice for LCOE prediction in the HRES, as indicated by the response plot, and predicted versus actual LCOEs shown in Figs. 14 and 15, respectively. Model hyperparameters of neural network models for LCOE are provided in Table 4.

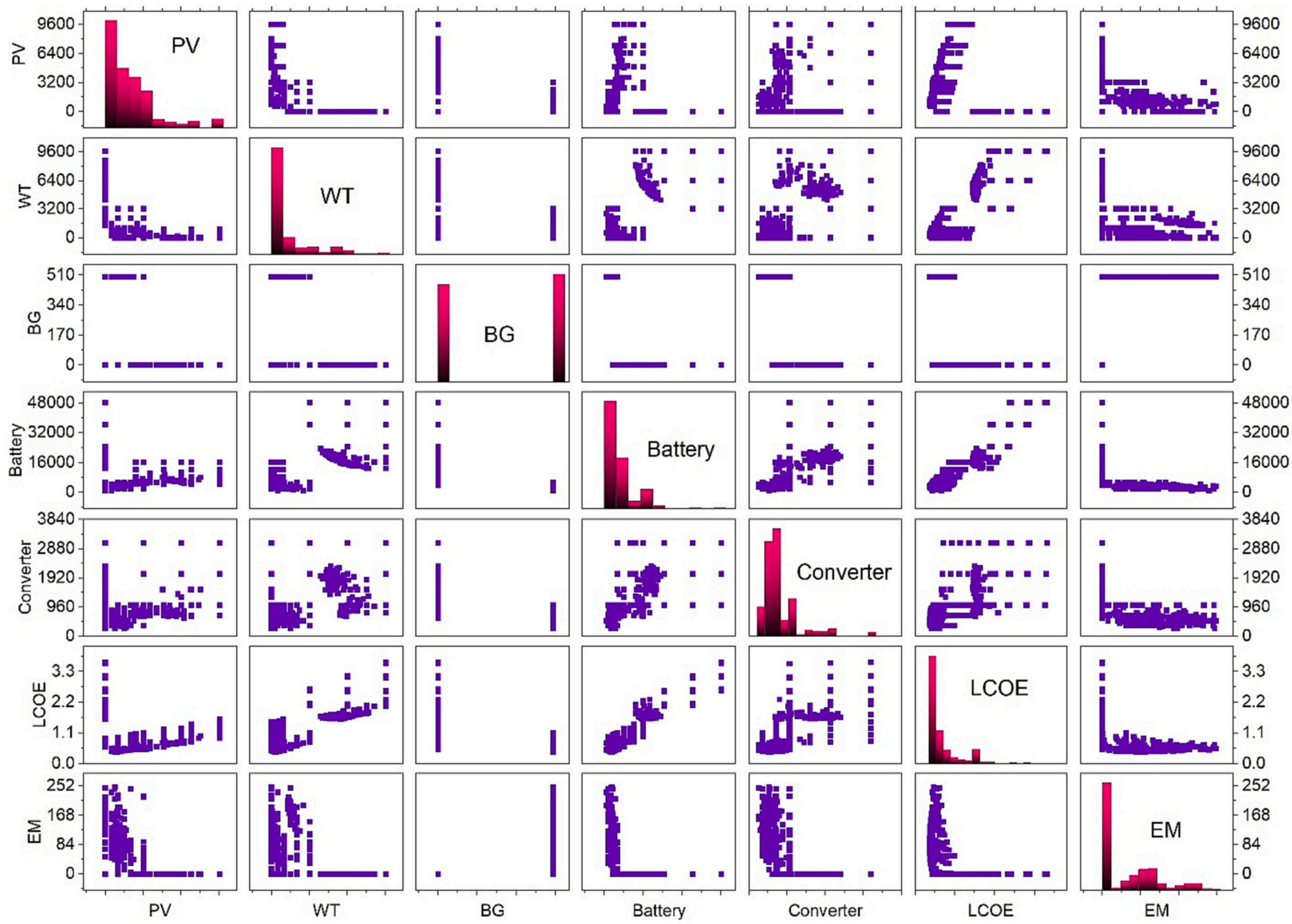

Fig. 13. Scatter matrix plot.

Table 3
Prediction of LCOE of the models through multiple ML techniques.

Regression Types	Training algorithms	RMSE	R^2	MSE	MAE	Training time (in *sec*)
Linear Regression	Linear	0.0385	0.99	0.0014822	0.025078	5.8596
Linear Regression	Interaction Linear	0.03058	1	0.00093514	0.019588	5.9103
Linear Regression	Robust Linear	0.041612	0.99	0.0017316	0.022055	5.0791
Stepwise Linear Regression	Stepwise Regression	0.030638	1	0.00093869	0.019492	10.525
Tree	Fine Tree	0.070794	0.98	0.0050118	0.02672	5.4198
Tree	Medium Tree	0.087925	0.97	0.0077309	0.036321	4.8752
Tree	Coarse Tree	0.145	0.91	0.021026	0.062793	4.4008
SVM	Linear SVM	0.039785	0.99	0.0015828	0.028207	4.0177
SVM	Quadratic SVM	0.033145	1	0.0010986	0.024936	83.369
SVM	Cubic SVM	0.09165	0.96	0.0083997	0.046573	90.384
SVM	Fine Gaussian SVM	0.2461	0.74	0.060564	0.060285	2.9018
SVM	Medium Gaussian SVM	0.10151	0.96	0.010304	0.030526	2.6133
SVM	Coarse Gaussian SVM	0.048526	0.99	0.0023548	0.029547	2.3184
Ensemble	Boosted Trees	0.067437	0.98	0.0045478	0.038154	6.1176
Ensemble	Bagged Trees	0.087238	0.97	0.0076104	0.035493	4.8175
Gaussian Process Regression	Squared Exponential GPR	0.075363	0.98	0.0056796	0.01226	36.945
Gaussian Process Regression	Matern 5/2 GPR	0.022737	1	0.00051695	0.0045933	34.124
Gaussian Process Regression	Exponential GPR	0.014287	1	0.00020412	0.004517	42.856
Gaussian Process Regression	Rational Quadratic GPR	0.020063	1	0.0040253	0.0045437	53.016
Neural Network	Narrow Neural Network	0.011605	1	0.00013468	0.0056936	7.7455
Neural Network	Medium Neural Network	0.0088319	1	7.8002e-05	0.0039739	9.131
Neural Network	Wide Neural Network	0.0080785	1	6.5262e-05	0.0036875	18.203
Neural Network	Bilayered Neural Network	0.0074143	1	5.4972e-05	0.0034191	15.387
Neural Network	Trilayered Neural Network	0.0092423	1	8.5419e-05	0.0043468	23.224
Kernel	SVM Kernel	0.25074	0.73	0.06287	0.078402	19.782
Kernel	Least Squares Regression Kernel	0.27034	0.68	0.073086	0.11727	19.685

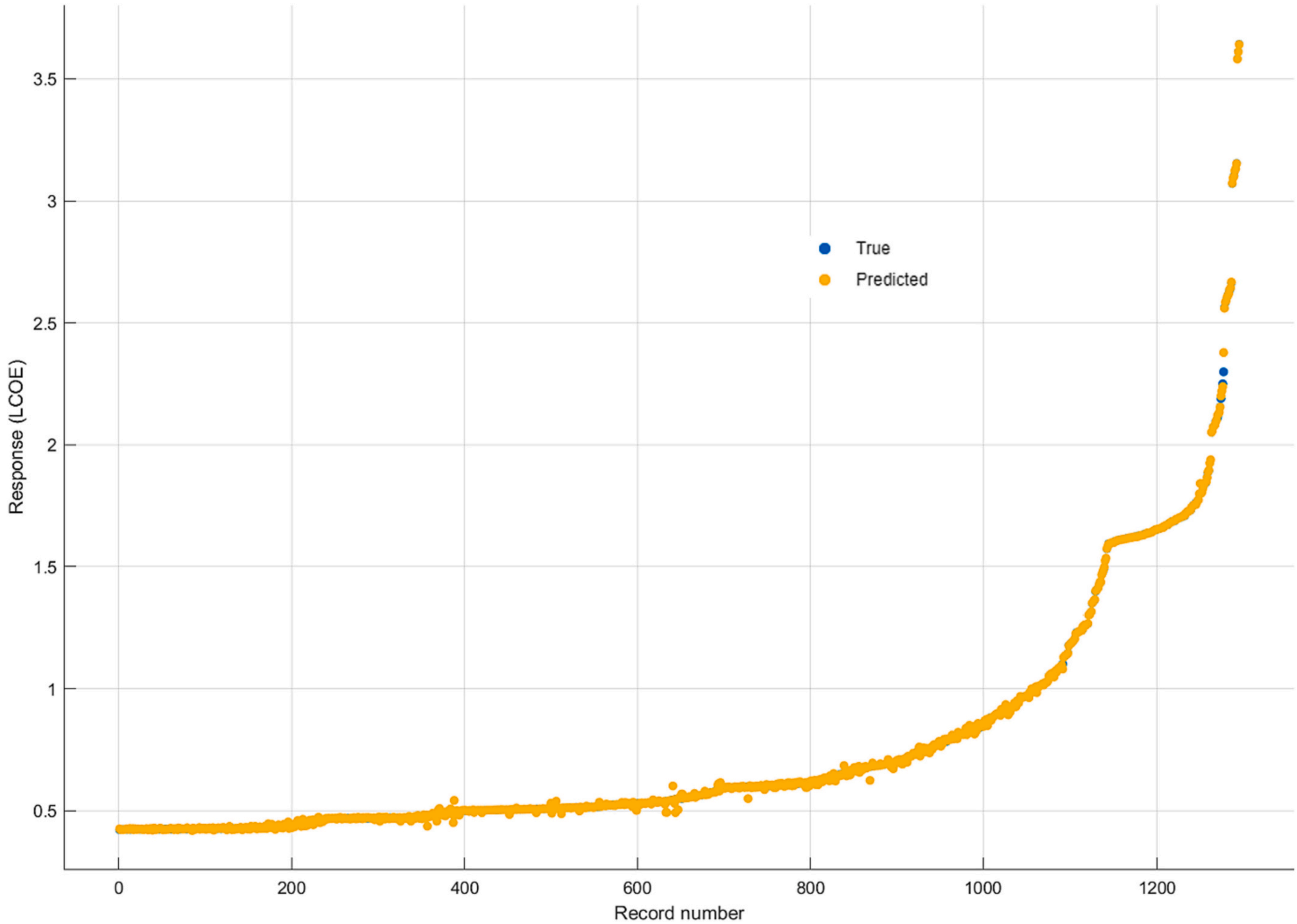

Fig. 14. Response plot using Bilayered Neural Network model for LCOE.

3.4.2. CO_2 emissions prediction using machine learning models

A total of 26 machine learning algorithms of different types were employed to develop a predictive model for estimating CO_2 emissions (EM). Furthermore, to prevent overfitting, a 5-fold cross-validation scheme has been employed. The results are presented in Table 5. The majority of machine learning techniques used to predict EM show strong agreement with simulation data. Linear Regression, Tree, Ensemble, Neural Network, and Kernel regression models demonstrate relatively quick training times compared to other methods, taking a maximum of 20.028 s to train. In contrast, the Cubic SVM training algorithm requires the longest training duration, taking 85.497 s. Gaussian Process Regression models range between 34.236 and 50.889 s for training. Among all models, the Medium Gaussian SVM exhibits the shortest training time, completing in just 0.61993 s.

The accuracy of EM prediction improves with the use of Neural Network models, specifically the Rational Quadratic GPR, Medium Neural Network, and Wide Neural Network. These models demonstrate a coefficient of determination of 1, indicating high accuracy. The Medium Neural Network model outperforms the others in terms of RMSE, MSE, and MAE, with values of 3.5409, 12.538, and 1.6295, respectively. Therefore, the Medium Neural Network model is considered the most suitable choice for EM prediction as indicated by the response plot and the predicted versus actual EMs shown in Figs. 16 and 17, respectively. Model hyperparameters of neural network models for EM are provided in Table 6.

3.5. Comparisons with previous studies

Table 7 compares the LCOE of the optimised combination from present study with the LCOE of renewable energy systems with energy storage from previous studies. It is found that the LCOE of different systems varies considerably with the combination of renewable energy sources and their installation capacity. The lowest LCOE from present study, i.e., 0.4224 $/kWh is clearly higher than the price of electricity for systems which are in the size of MW. This is mainly due to the energy systems in larger size can produce more electricity, which reduces the LCOE. As the BG is used in this study, the price of biomass feedstock undoubtedly accounts for a large portion of the total capital cost, increasing the LCOE. In addition, higher LCOE is related to the complexity of energy systems, as concluded by the comparison between the LCOE from this study and study in [47]. The investment cost considered for installing more energy storage systems would be higher and increase the LCOE. It should be noted that even the lowest LCOE derived from present study is significantly higher than the typical tariff for residential electricity in India (around 0.078 $/kWh [48]). Therefore, scaling up the capacity and reducing feedstock cost are key factors in promoting implementation of HRES, as one of the main objectives of HRES is to obtain the comparable electricity price to achieve reliability for its use.

4. Conclusions

This article offers an extensive examination of the technical, financial, and environmental aspects of HRESs designed to provide 100%

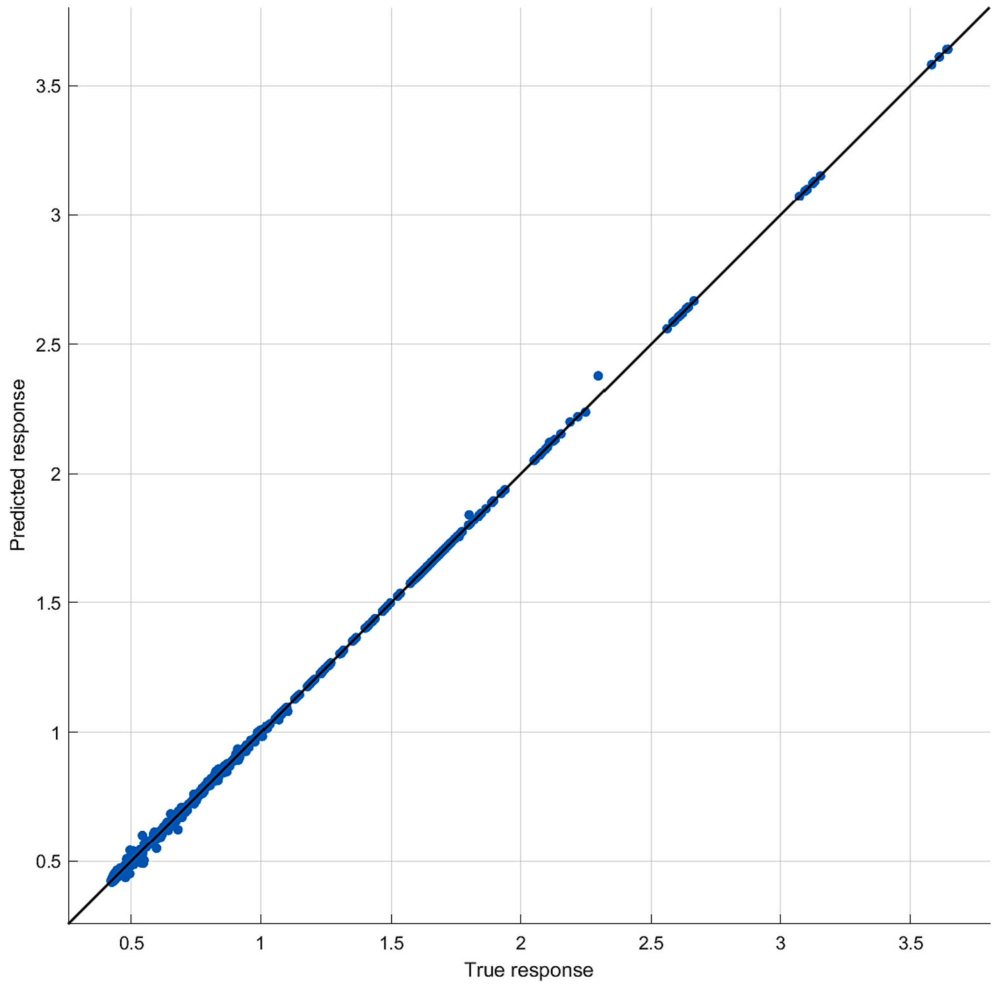

Fig. 15. Predicted LCOE versus the actual LCOE using Bilayered Neural Network model.

Table 4
Model hyperparameters of neural network models for LCOE.

Neural network model	Activation function	Model hyperparameters
Narrow Neural Network	ReLU	Number of fully connected layer:1 First layer size:10 Iteration limit:1000
Medium Neural Network	ReLU	Number of fully connected layer:1 First layer size:25 Iteration limit:1000
Wide Neural Network	ReLU	Number of fully connected layer:1 First layer size:100 Iteration limit:1000
Bilayered Neural Network	ReLU	Number of fully connected layer:2 First layer size:10 Second layer size:10 Iteration limit:1000
Trilayered Neural Network	ReLU	Number of fully connected layer:3 First layer size:10 Second layer size:10 Third layer size:10 Iteration limit:1000

renewable electricity exclusively to a remote location, i.e., Henry Island in India. Four combinations involving photovoltaic panels, wind turbines, biogas generators, batteries, and converters were explored and optimised based on techno-economic considerations. Additionally, machine learning techniques are employed to analyse economic and environmental performance data for up to 1295 combinations. The main findings derived from this research can be summarised as follows:

- Regarding surplus electricity output, System C with a combination of wind turbine, photovoltaic panel, convertor and battery yields the maximum (2,838,968 kWh/yr), while System A with a combination of wind turbine, photovoltaic panel, biogas generator, convertor and battery yield the minimum.
- The economic results indicate that System A, consisting of wind turbine, photovoltaic panel, biogas generator, convertor and battery, has the lowest levelized cost of electricity (LCOE) at $0.4224/kWh and net present cost (NPC) of $6.41 million among all the systems examined. On the other hand, System D, comprising wind turbine, battery, biogas generator, and convertor, exhibits the highest LCOE ($0.5947/kWh) and NPC ($9.02 million) among all the configurations investigated.
- The environmental analysis reveals that System C, which does not include biogas generator would emit zero CO_2 whereas System D has the highest CO_2 emissions.
- For LCOE prediction, the Bilayered Neural Network model achieves the highest accuracy among all training algorithms, with an impressive R^2 value of 1. Additionally, it achieves the lowest values for root mean square error (RMSE), mean squared error (MSE), and mean absolute error (MAE), which are recorded as 7.4143×10^{-3}, 5.4972×10^{-5}, and 3.4191×10^{-3}, respectively.

Table 5
Evaluation of EM prediction models employing diverse ML techniques.

Regression Types	Training algorithms	RMSE	R^2	MSE	MAE	Training time (in sec)
Linear Regression	Linear	40.02	0.65	1601.6	26.869	3.2417
Linear Regression	Interaction Linear	30.883	0.79	953.77	20.02	2.627
Linear Regression	Robust Linear	43.588	0.58	1899.9	23.572	2.0126
Stepwise Linear Regression	Stepwise Regression	30.914	0.79	955.65	19.885	2.9907
Tree	Fine Tree	12.844	0.96	164.97	5.6704	1.1266
Tree	Medium Tree	15.754	0.95	248.18	7.09	0.91839
Tree	Coarse Tree	22.347	0.89	499.37	11.225	4.7272
SVM	Linear SVM	40.974	0.63	1678.8	24.938	4.047
SVM	Quadratic SVM	31.746	0.78	1007.8	20.732	43.674
SVM	Cubic SVM	156.39	−4.37	24,459	80.445	85.497
SVM	Fine Gaussian SVM	15.753	0.95	248.14	9.3891	0.91913
SVM	Medium Gaussian SVM	25.84	0.85	667.73	15.341	0.61993
SVM	Coarse Gaussian SVM	36.979	0.70	1367.4	22.837	1.5349
Ensemble	Boosted Trees	12.814	0.96	164.19	6.4671	2.2583
Ensemble	Bagged Trees	16.246	0.94	263.93	7.4849	5.2403
Gaussian Process Regression	Squared Exponential GPR	10.11	0.98	102.2	4.1125	36.454
Gaussian Process Regression	Matern 5/2 GPR	5.9987	0.99	35.984	1.9724	44.031
Gaussian Process Regression	Exponential GPR	6.4029	0.99	40.997	2.3557	34.236
Gaussian Process Regression	Rational Quadratic GPR	4.0145	1	16.117	1.4748	50.889
Neural Network	Narrow Neural Network	6.7814	0.99	45.987	3.049	4.584
Neural Network	Medium Neural Network	3.5409	1	12.538	1.6295	8.6323
Neural Network	Wide Neural Network	4.0238	1	16.191	1.324	14.514
Neural Network	Bilayered Neural Network	6.4135	0.99	41.133	2.7852	14.162
Neural Network	Trilayered Neural Network	7.4303	0.99	55.209	3.4088	20.028
Kernel	SVM Kernel	47.799	0.50	2284.7	28.902	15.052
Kernel	Least Squares Regression Kernel	25.263	0.86	638.24	14.906	14.659

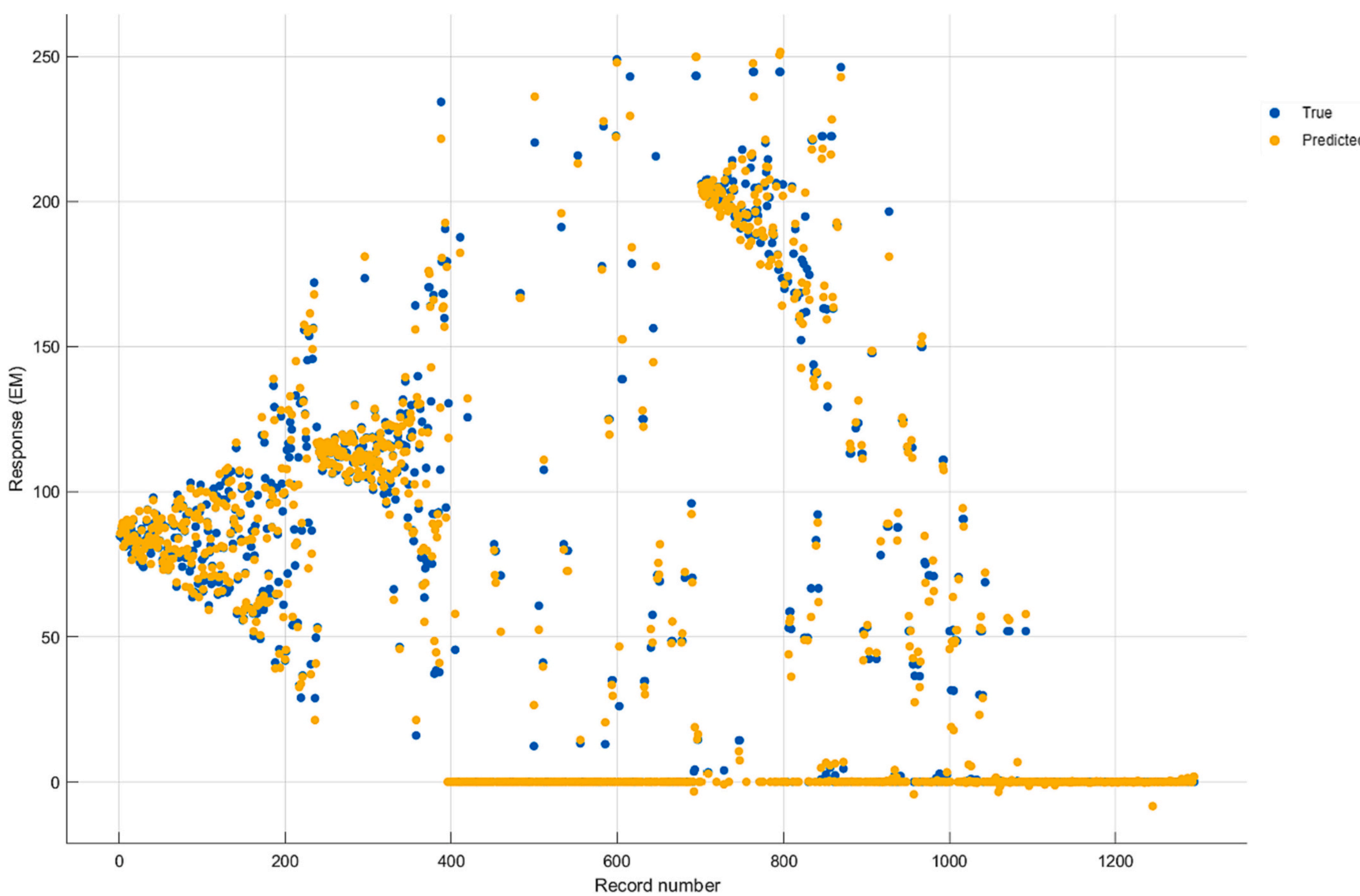

Fig. 16. Response plot using medium neural network model for EM.

- For CO_2 emission prediction, the Medium Neural Network model outperforms the others in terms of R^2, RMSE, MSE, and MAE, with values of 1, 3.5409, 12.538, and 1.6295, respectively. Therefore, the Medium Neural Network model is considered the most suitable choice for CO_2 emission prediction.

This study addresses a critical gap in the existing literature by

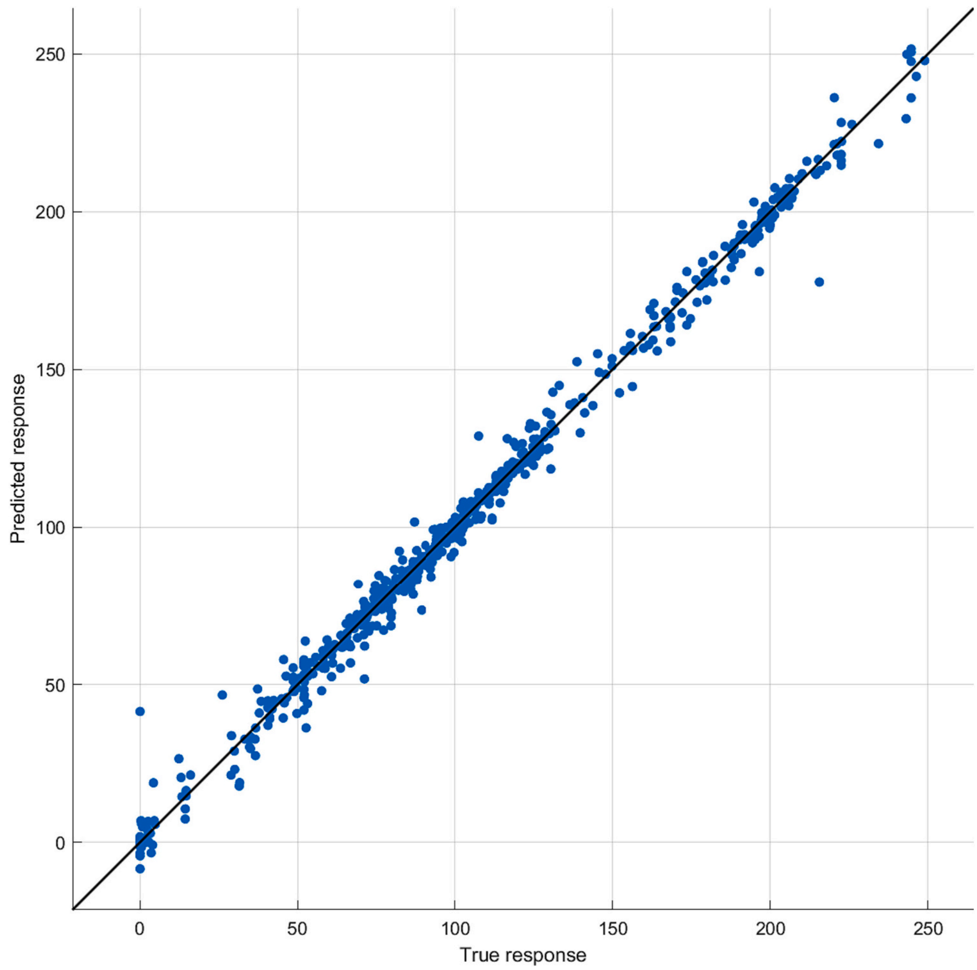

Fig. 17. Predicted EM versus the actual EM using medium neural network model with 5-fold cross validation.

Table 6
Model hyperparameters of neural network models for EM.

Neural network model	Activation function	Model hyperparameters
Narrow Neural Network	ReLU	Number of fully connected layer:1 First layer size:10 Iteration limit:1000
Medium Neural Network	ReLU	Number of fully connected layer:1 First layer size:25 Iteration limit:1000
Wide Neural Network	ReLU	Number of fully connected layer:1 First layer size:100 Iteration limit:1000
Bilayered Neural Network	ReLU	Number of fully connected layer:2 First layer size:10 Second layer size:10 Iteration limit:1000
Trilayered Neural Network	ReLU	Number of fully connected layer:3 First layer size:10 Second layer size:10 Third layer size:10 Iteration limit:1000

Table 7
Comparative performances with previous studies.

Renewable energy systems	Capacity	Energy storage	LCOE ($/kWh)	Reference
Stand-alone PV	125 MW	Electrolyser and fuel cell	0.0702	[49]
Stand-alone WT	34.5 MW		0.0786	
Hybrid PV and WT	PV: 2 MW WT: 30.5 MW		0.0783	
Stand-alone PV	1707 kW	Electrolyser and battery	0.68	[47]
Stand-alone WT	3000 kW	Electrolyser, fuel cell, and battery	0.88	
Hybrid PV and WT	PV: 985 kW WT: 1500 kW	Electrolyser and battery	0.66	
Hybrid PV and BG	PV: 80 kW BG: 80 kW	Grid	0.488	[50]
Hybrid PV, WT, and BG	PV:1.79 MW WT:2 MW BG: 0.92 MW	Battery and pumped-hydro storage	0.1626	[51]
Hybrid PV, WT, and BG	PV:937 kW WT:340 kW BG: 500 kW	Battery	0.4224	Present study

examining the performance of off-grid HRES that rely solely on 100% renewable energy sources, leveraging machine learning techniques. In addition to shedding light on system performance, the study offers valuable insights into optimised configurations and predictive models for a thorough techno-economic and environmental evaluation. The identified optimised hybrid system emerges as a promising solution for rural and remote areas in India. The employed methodology is straightforward, facilitating its application to similar HRES studies across diverse geographical locations. However, to provide a more comprehensive view of the system, a thorough resilience assessment of the proposed HRES is crucial. Furthermore, investigating the resilience of stand-alone microgrids during natural disasters in future work will contribute to a more robust understanding of the system's capabilities and vulnerabilities across various operational scenarios.

CRediT authorship contribution statement

Dibyendu Roy: Writing – original draft, Methodology, Investigation, Formal analysis, Conceptualization, Software, Data Curation, Writing - Review & Editing. **Shunmin Zhu:** Writing – review & editing, Visualization, Validation, Investigation. **Ruiqi Wang:** Writing – review & editing, Validation. **Pradip Mondal:** Writing – review & editing, Software, Methodology, Investigation. **Janie Ling-Chin:** Writing – review & editing, Project administration. **Anthony Paul Roskilly:** Supervision, Resources, Project administration, Funding acquisition.

Declaration of competing interest

The authors declare that they have no known competing financial interests or personal relationships that could have appeared to influence the work reported in this paper.

Data availability

Data will be made available on request.

Acknowledgments

This research work was funded by the Engineering and Physical Science Research Council of UK (Grant numbers: EP/T022949/1). For the purpose of Open Access, the authors have applied a CC BY public copyright licence to any Author Accepted Manuscript version arising from this submission.

Appendix A

Table A1
Electric demand at the study location.

Load	Appliances	Quantity	Power (W)	Summer (Mar-Oct)			Winter (Nov-Feb)		
				Usage (hr)	Load (Wh/d)	Total category (kWh/d)	Usage (hr)	Load (Wh/d)	Total category (kWh/d)
House demand (1)	CFL	3	40	7	840		7	840	
	Fan	2	70	8	1120		0	0	
	Television	1	100	5	500		5	500	
	Mobile Charger	1	10	1	10		1	10	
	Miscellaneous	1	100	1	100		1	100	
Total number of houses (1600)						4112			2320

Table A2
Technoeconomic specifications of components.

Component	Parameters	Data	**Ref**
PV	Rated capacity	1 kW	[52,53]
	Derating factor	80%	
	Rated voltage	54.7 V	
	Temperature coefficient	-0.5%/°C	
	Efficiency	13%	
	Operating Temperature	47 °C	
	Rated current	5.98 A	
	Efficiency	13%	
	Capital cost	$925/kW	
	Replacement cost	$800/kW	
	O&M cost	$15/kW	
	Lifetime	25	
WT	Power rating	1 kW	[54,55]
	Hub height	20 m	
	Rated wind speed	12.5 m/s	
	Start-up wind speed	2.5 m/s	
	Nominal voltage configuration	24 V/48 V	
	Diameter of rotor	3.35 m	
	Capital cost	$1980/kW	
	Replacement cost	$980/kW	
	O&M cost	$25/year	
	Lifetime	25 years	
Battery	Voltage rating	12 V	[53]
	Capacity ratio	0.403	
	Roundtrip efficiency	80%	
	Maximum charge current	16.7 A	

(continued on next page)

Table A2 (*continued*)

Component	Parameters	Data	**Ref**
	Maximum discharge current	24.3 A	
	Minimum state of charge	40%	
	Initial state of charge	100%	
	Capital cost	$240 per unit	
	Replacement cost	$190 per unit	
	O&M cost	$2.0 per year	
	Lifetime	5 years	
Converter	Power rating	1 kW	[38,56,57]
	Inverter efficiency	95%	
	Rectifier efficiency	95%	
	Capital cost	$300/kW	
	Replacement cost	$300/kW	
	O&M cost	3$/year	
	Lifetime	15 years	
BG	Power rating	500 kW	[50,58]
	Minimum load ratio	50%	
	Fuel cost	100$/t	
	Biogas LHV	5.5 MJ/kg	
	Biogas density	0.720 kg/m^3	
	Capital cost	$3000/unit	
	Replacement cost	$1250/unit	
	O&M cost	0.10$/hour	
	Lifetime	20,000 h	

References

[1] IEA. India energy outlook. 2021.
[2] Sachs, Jeffrey D, Lafortune Guillaume, Fuller Grayson, Drumm E. Sustainable development report. Ireland. 2023.
[3] PIB. Mission 500 GW by 2030. PIB,Government of India; 2021. p. 2–3.
[4] PIB. Cabinet Approves India's Updated Nationally Determined Contribution to be Communicated to the United Nations Framework Convention on Climate Change. Gov India; 2022.
[5] Das S, De S. Technically efficient, economic and environmentally benign hybrid decentralized energy solution for an Indian village: multi criteria decision making approach. J Clean Prod 2023;388:135717. https://doi.org/10.1016/j.jclepro.2022.135717.
[6] Abdelhady S. Techno-economic study and the optimal hybrid renewable energy system design for a hotel building with net zero energy and net zero carbon emissions. Energy Convers Manag 2023;289:117195. https://doi.org/10.1016/j.enconman.2023.117195.
[7] Das S, Ray A, De S. Comparative analysis of storage modules under different dispatch strategies for an optimum decentralized hybrid energy solution: a case study of a remote Indian village. Clean Techn Environ Policy 2022;24:2495–515. https://doi.org/10.1007/s10098-022-02330-0.
[8] Ngila A, Farzaneh H. Energy conversion and management: X techno-economic analysis and dynamic power simulation of a hybrid solar-wind-battery-flywheel system for off-grid power supply in remote areas in Kenya introduction. Energy Convers Manag X 2023;18:100381. https://doi.org/10.1016/j.ecmx.2023.100381.
[9] Ahmed EEE, Demirci A, Tercan SM. Optimal sizing and techno-enviro-economic feasibility assessment of solar tracker-based hybrid energy systems for rural electrification in Sudan. Renew Energy 2023;205:1057–70. https://doi.org/10.1016/j.renene.2023.02.022.
[10] Das S, De S. MCDM for simultaneous optimum economy, investment risk and environmental impact for distributed renewable power: demonstration with an Indian village data. Energy Convers Manag 2023;277:116631. https://doi.org/10.1016/j.enconman.2022.116631.
[11] Ma T, Javed MS. Integrated sizing of hybrid PV-wind-battery system for remote island considering the saturation of each renewable energy resource. Energy Convers Manag 2019;182:178–90. https://doi.org/10.1016/j.enconman.2018.12.059.
[12] Skroufouta S, Baltas E. Investigation of hybrid renewable energy system (HRES) for covering energy and water needs on the island of Karpathos in Aegean Sea. Renew Energy 2021;173:141–50. https://doi.org/10.1016/j.renene.2021.03.113.
[13] Yazdani H, Baneshi M, Yaghoubi M. Techno-economic and environmental design of hybrid energy systems using multi-objective optimization and multi-criteria decision making methods. Energy Convers Manag 2023;282:116873. https://doi.org/10.1016/j.enconman.2023.116873.
[14] Hosseini Dehshiri SS, Firoozabadi B. Comparison, evaluation and prioritization of solar photovoltaic tracking systems using multi criteria decision making methods. Sustain Energy Technol Assessm 2023;55:102989. https://doi.org/10.1016/j.seta.2022.102989.
[15] Qiao Z, Li L, Zhao X, Liu L, Zhang Q, Hechmi S, et al. An enhanced Runge Kutta boosted machine learning framework for medical diagnosis. Comput Biol Med 2023;160:106949. https://doi.org/10.1016/j.compbiomed.2023.106949.
[16] Liao J, Hu J, Yan F, Chen P, Zhu L, Zhou Q. A comparative investigation of advanced machine learning methods for predicting transient emission characteristic of diesel engine. Root Sum Squares 2023;350. https://doi.org/10.1016/j.fuel.2023.128767.
[17] Bluwstein K, Buckmann M, Joseph A. Credit growth, the yield curve and financial crisis prediction: evidence from a machine learning approach. J Int Econ 2023:103773. https://doi.org/10.1016/j.jinteco.2023.103773.
[18] Kwekha-Rashid AS, Abduljabbar HN, Alhayani B. Coronavirus disease (COVID-19) cases analysis using machine-learning applications. Appl Nanosci 2023;13:2013–25. https://doi.org/10.1007/s13204-021-01868-7.
[19] Xu Z, Mohsin M, Ullah K, Ma X. Using econometric and machine learning models to forecast crude oil prices: insights from economic history. Res Policy 2023;83:103614. https://doi.org/10.1016/j.resourpol.2023.103614.
[20] Tamjid Shabestari S, Kasaeian A, Vaziri Rad MA, Forootan Fard H, Yan WM, Pourfayaz F. Techno-financial evaluation of a hybrid renewable solution for supplying the predicted power outages by machine learning methods in rural areas. Renew Energy 2022;194:1303–25. https://doi.org/10.1016/j.renene.2022.05.160.
[21] Roy D. Modelling an off-grid hybrid renewable energy system to deliver electricity to a remote Indian island. Energy Convers Manag 2023;281:116839. https://doi.org/10.1016/j.enconman.2023.116839.
[22] Izadi A, Shahafve M, Ahmadi P. Neural network genetic algorithm optimization of a transient hybrid renewable energy system with solar/wind and hydrogen storage system for zero energy buildings at various climate conditions. Energy Convers Manag 2022;260:115593. https://doi.org/10.1016/j.enconman.2022.115593.
[23] Sakthi U, Anil Kumar T, Vimala Kumar K, Qamar S, Kumar Sharma G, Azeem A. Power grid based renewable energy analysis by photovoltaic cell machine learning architecture in wind energy hybridization. Sustain Energy Technol Assessm 2023;57:103243. https://doi.org/10.1016/j.seta.2023.103243.
[24] Ghandehariun S, Ghandehariun AM, Ziabari NB. Performance prediction and optimization of a hybrid renewable-energy-based multigeneration system using machine learning. Energy 2023;282:128908. https://doi.org/10.1016/j.energy.2023.128908.
[25] Al Afif R, Ayed Y, Maaitah ON. Feasibility and optimal sizing analysis of hybrid renewable energy systems: a case study of Al-Karak, Jordan. Renew Energy 2023;204:229–49. https://doi.org/10.1016/j.renene.2022.12.109.
[26] Ramesh M, Saini RP. Dispatch strategies based performance analysis of a hybrid renewable energy system for a remote rural area in India. J Clean Prod 2020;259:120697. https://doi.org/10.1016/j.jclepro.2020.120697.
[27] He B, Ismail N, Leng KKK, Chen G. Techno-economic analysis of an HRES with fuel cells, solar panels, and wind turbines using an improved Al-Biruni algorithm. Heliyon 2023;9:e22828. https://doi.org/10.1016/j.heliyon.2023.e22828.
[28] Keyvandarian A, Saif A. Optimal sizing of a reliability-constrained, stand-alone hybrid renewable energy system using robust satisficing. Renew Energy 2023;204:569–79. https://doi.org/10.1016/j.renene.2023.01.036.
[29] Pourmohammadi P, Saif A. Robust metamodel-based simulation-optimization approaches for designing hybrid renewable energy systems. Appl Energy 2023;341:121132. https://doi.org/10.1016/j.apenergy.2023.121132.
[30] Goh QH, Zhang L, Ho YK, Chew IML. Modelling and multi-objective optimisation of sustainable solar-biomass-based hydrogen and electricity co-supply hub using metaheuristic-TOPSIS approach. Energy Convers Manag 2023;293:117484. https://doi.org/10.1016/j.enconman.2023.117484.
[31] Maleki Tehrani M, Akhtari M, Kasaeian A, Vaziri Rad MA, Toopshekan A, Sadeghi Motlagh M. Techno-economic investigation of a hybrid biomass renewable energy system to achieve the goals of SDG-17 in deprived areas of Iran. Energy

Convers Manag 2023;291:117319. https://doi.org/10.1016/j.enconman.2023.117319.
[32] Kumar N, Namrata K, Samadhiya A. Techno socio-economic analysis and stratified assessment of hybrid renewable energy systems for electrification of rural community. Sustain Energy Technol Assessm 2023;55:102950. https://doi.org/10.1016/j.seta.2022.102950.
[33] Kilic M, Altun AF. Dynamic modelling and multi-objective optimization of off-grid hybrid energy systems by using battery or hydrogen storage for different climates. Int J Hydrog Energy 2023;48:22834–54. https://doi.org/10.1016/j.ijhydene.2022.12.103.
[34] Abdullah HM, Park S, Seong K, Lee S. Hybrid renewable energy system design: a machine learning approach for optimal sizing with net-metering costs. Sustain 2023:15. https://doi.org/10.3390/su15118538.
[35] Census India. Henry'S Island Village population - Namkhana. West Bengal: South Twenty Four Parganas; 2011.
[36] NASA. NASA Prediction of Worldwide Energy Resourse (POWER) database. 2024.
[37] Page J. The role of solar-radiation climatology in the design of photovoltaic systems. Elsevier Ltd; 2018. https://doi.org/10.1016/B978-0-12-809921-6.00016-1.
[38] Kumar R, Channi HK. A PV-biomass off-grid hybrid renewable energy system (HRES) for rural electrification: design, optimization and techno-economic-environmental analysis. J Clean Prod 2022;349:131347. https://doi.org/10.1016/j.jclepro.2022.131347.
[39] Mousavi SA, Zarchi RA, Astaraei FR, Ghasempour R, Khaninezhad FM. Decision-making between renewable energy configurations and grid extension to simultaneously supply electrical power and fresh water in remote villages for five different climate zones. J Clean Prod 2021;279:123617. https://doi.org/10.1016/j.jclepro.2020.123617.
[40] Luta DN, Raji AK. Decision-making between a grid extension and a rural renewable off-grid system with hydrogen generation. Int J Hydrog Energy 2018;43:9535–48. https://doi.org/10.1016/j.ijhydene.2018.04.032.
[41] Alsagri AS, Alrobaian AA, Nejlaoui M. Techno-economic evaluation of an off-grid health clinic considering the current and future energy challenges: a rural case study. Renew Energy 2021;169:34–52. https://doi.org/10.1016/j.renene.2021.01.017.
[42] Sifakis N, Konidakis S, Tsoutsos T. Hybrid renewable energy system optimum design and smart dispatch for nearly zero energy ports. J Clean Prod 2021;310:127397. https://doi.org/10.1016/j.jclepro.2021.127397.
[43] Kumar S, Koteswara Rao S. Optimum capacity of hybrid renewable energy system suitable for fulfilling yearly load demand for a community building located at Vaddeswaram. Andhra Pradesh Energy Build 2022;277:112570. https://doi.org/10.1016/j.enbuild.2022.112570.
[44] Elmorshedy MF, Elkadeem MR, Kotb KM, Taha IBM, Mazzeo D. Optimal design and energy management of an isolated fully renewable energy system integrating batteries and supercapacitors. Energy Convers Manag 2021;245:114584. https://doi.org/10.1016/j.enconman.2021.114584.
[45] Zhu S, Wang K, González-Pino I, Song J, Yu G, Luo E, et al. Techno-economic analysis of a combined heat and power system integrating hybrid photovoltaic-thermal collectors, a Stirling engine and energy storage. Energy Convers Manag 2023:284. https://doi.org/10.1016/j.enconman.2023.116968.
[46] Cai J, Xu K, Zhu Y, Hu F, Li L. Prediction and analysis of net ecosystem carbon exchange based on gradient boosting regression and random forest. Appl Energy 2020;262:114566. https://doi.org/10.1016/j.apenergy.2020.114566.
[47] Abdin Z, Mérida W. Hybrid energy systems for off-grid power supply and hydrogen production based on renewable energy: a techno-economic analysis. Energy Convers Manag 2019;196:1068–79. https://doi.org/10.1016/j.enconman.2019.06.068.
[48] www.GlobalPetrolPrices.com. India electricity prices. 2024.
[49] Oyewole OL, Nwulu NI, Okampo EJ. Optimal design of hydrogen-based storage with a hybrid renewable energy system considering economic and environmental uncertainties. Energy Convers Manag 2024;300:117991. https://doi.org/10.1016/j.enconman.2023.117991.
[50] Ribó-Pérez D, Herraiz-Cañete Á, Alfonso-Solar D, Vargas-Salgado C, Gómez-Navarro T. Modelling biomass gasifiers in hybrid renewable energy microgrids; a complete procedure for enabling gasifiers simulation in HOMER. Renew Energy 2021;174:501–12. https://doi.org/10.1016/j.renene.2021.04.083.
[51] Al-Ghussain L, Darwish Ahmad A, Abubaker AM, Mohamed MA. An integrated photovoltaic/wind/biomass and hybrid energy storage systems towards 100% renewable energy microgrids in university campuses. Sustain Energy Technol Assessm 2021;46:101273. https://doi.org/10.1016/j.seta.2021.101273.
[52] Akhtari MR, Shayegh I, Karimi N. Techno-economic assessment and optimization of a hybrid renewable earth - air heat exchanger coupled with electric boiler, hydrogen, wind and PV configurations. Renew Energy 2020;148:839–51. https://doi.org/10.1016/j.renene.2019.10.169.
[53] Khan FA, Pal N, Saeed SH, Yadav A. Modelling and techno-economic analysis of standalone SPV/wind hybrid renewable energy system with lead-acid battery technology for rural applications. J Energy Storage 2022;55:105742. https://doi.org/10.1016/j.est.2022.105742.
[54] Liu J, Jian L, Wang W, Qiu Z, Zhang J, Dastbaz P. The role of energy storage systems in resilience enhancement of health care centers with critical loads. J Energy Storage 2021;33:102086. https://doi.org/10.1016/j.est.2020.102086.
[55] Khan FA, Pal N, Saeed SH, Yadav A. Techno-economic and feasibility assessment of standalone solar photovoltaic/wind hybrid energy system for various storage techniques and different rural locations in India. Energy Convers Manag 2022;270:116217. https://doi.org/10.1016/j.enconman.2022.116217.
[56] Nallolla CA, Perumal V. Optimal design of a hybrid off-grid renewable energy system using techno-economic and sensitivity analysis for a rural remote location. Sustain 2022:14. https://doi.org/10.3390/su142215393.
[57] Kushwaha PK, Bhattacharjee C. Integrated techno-economic-enviro-socio design of the hybrid renewable energy system with suitable dispatch strategy for domestic and telecommunication load across India. J Energy Storage 2022;55:105340. https://doi.org/10.1016/j.est.2022.105340.
[58] Konneh KV, Adewuyi OB, Gamil MM, Fazli AM, Senjyu T. A scenario-based multi-attribute decision making approach for optimal design of a hybrid off-grid system. Energy 2023;265:125663. https://doi.org/10.1016/j.energy.2022.125663.